ACTA ABP BIOCHIMICA POLONICA

Vol. 70, No 4/2023
875–884
https://doi.org/10.18388/abp.2020_6722

Regular paper

# A novel ferroptosis-related gene signature associated with cuproptosis for predicting overall survival in breast cancer patients

Xiaoyu Zhang[1] and Qunchen Zhang[2]

[1]Department of Thoracic Surgery, The First Affiliated Hospital of Shantou University Medical College, Shantou City, Guangdong Province, P.R. China; [2]Department of Breast, Jiangmen Central Hospital, Jiangmen City, Guangdong Province, P.R. China

**Purpose** Ferroptosis and cuproptosis are both metal-dependent regulated cell death that play an important role in cancer. However, the expression patterns and the prognostic values of ferroptosis-related genes (FRGs) associated with cuproptosis in breast cancer (BC) are largely unknown. This study aims to explore the prognostic value of cuproptosis-related FRGs and their relationship with tumor microenvironments in BC. **Methods** The clinical and RNA sequencing data of BC patients from TCGA, METABRIC and GEO databases were analyzed. The least absolute shrinkage and selection operator regression analysis was used to establish prognostic signatures based on cuproptosis-related FRGs. The overall survival between risk subgroups was assessed by Kaplan-Meier analysis. The changes in risk score during neoadjuvant chemotherapy, and differences in immune cells, immune checkpoints, and drug sensitivity between risk subgroups were also analyzed in this study. **Results** A successful development of a prognostic signature based on cuproptosis-related FRGs in the TCGA cohort was achieved and it was validated in the METABRIC cohort. Gene set enrichment analysis results revealed the enrichment of steroid biosynthesis and ABC transporters in the high-risk group. Moreover, the signature was also found to be associated with immune cells and immune checkpoints. Lower risk score in patients after neoadjuvant chemotherapy and higher sensitivity of the high-risk group to AKT inhibitor VIII and cisplatin was also observed. **Conclusion** Cuproptosis-related FRGs can be used as a novel prognostic signature for predicting the overall survival of BC patients. This can provide meaningful insights into the selection of immunotherapy and antitumor drugs for BC.

**Keywords**: breast cancer, ferroptosis, cuproptosis, immune microenvironment, prognosis

**Received**: 06 March, 2023; revised: 15 August, 2023; accepted: 25 August, 2023; available on-line: 06 November, 2023

e-mail: qczhang2014@163.com

**Abbreviations**: BC, breast cancer; ER, estrogen receptor; FRGs, ferroptosis-related genes; HER-2, human epidermal growth factor receptor; GEO, gene expression omnibus; GO, gene ontology; GSEA, gene set enrichment analysis; IC50, half-maximal inhibitory concentration; KEGG, kyoto encyclopedia of genes and genomes; LASSO, least absolute shrinkage and selection operator; METABRIC, molecular taxonomy of breast cancer international consortium; OS, overall survival; PPI, protein-protein interaction; PR, progesterone receptor; ROC, receiver operating characteristic; TCGA, the cancer genome atlas.

## INTRODUCTION

Breast cancer (BC) is one of the most frequently diagnosed cancer in women worldwide, with an extremely high rate of mortality (Azamjah *et al.*, 2019). Its incidence and death rates have increased over recent years making it the second most common cause of mortality in women (DeSantis *et al.*, 2019). Its progressive impact on younger individuals is a cause of concern. Although the etiology and mechanism of BC are not completely understood, biological features including cell infiltration and genetic abnormalities are thought to be the major causes associated with the progression and metastasis of the disease (Feng *et al.*, 2018; Loibl *et al.*, 2021). Although there have been advancements in diagnosis, chemotherapy, endocrine and targeted therapies, the median survival in the case of advanced BC is only 31.8 months (Caswell-Jin *et al.*, 2018; Sung *et al.*, 2021). Early diagnosis and intervention are of paramount importance. Therefore, research on novel prognostic markers and therapeutic targets will provide improved opportunities for individualized treatment of BC.

Metals are essential components of metabolic processes. A significant portion of the proteases requires binding to metals, such as calcium, magnesium, iron, and copper for proper functioning (Waldron *et al.*, 2009). However, dysregulation of metal metabolism can lead to cell death. Ferroptosis, unlike apoptosis and autophagy, is an iron-dependent process of regulated cell death that is characterized by intracellular buildup of reactive oxygen species (ROS) and products of lipid peroxidation (Huang *et al.*, 2020). The primary mechanism of ferroptosis is the catalysis of the highly expressed unsaturated fatty acids on the cell membrane to produce liposome peroxidation, resulting in cell death, under the influence of divalent iron or ester oxygenase (Dixon *et al.*, 2012). Ferroptosis-related genes (FRGs) play an important role in the development of various cancers, including lung cancer, melanoma, renal cell carcinoma, BC, etc. (Friedmann Angeli *et al.*, 2019; Wang *et al.*, 2020; Zhao *et al.*, 2022). Activation of ferroptosis has been shown to prevent the growth and proliferation of tumors (Hassannia *et al.*, 2019). Therefore, ferroptosis can be a potential target for cancer therapy, especially in patients who have grown resistant to conventional forms of therapy (Hassannia *et al.*, 2019; Zhang *et al.*, 2022). For example, the sensitivity of triple-negative BC cells to gefitinib was enhanced by the inhibition of *GPX4* activation of Ferroptosis (Song *et al.*, 2020). Cuproptosis is a method of copper-induced regulated cell death. The direct interaction between copper ions and lipidated protein compo-

nents in the tricarboxylic acid cycle interferes with the iron-sulfur cluster proteins in the respiratory chain complex which ultimately leads to proteotoxic stress and cell death (Kahlson & Dixon, 2022). This could be another regulatory mechanism for the development of cancer (Jiang *et al.*, 2022). Iron-sulfur cluster proteins are able to maintain iron homeostasis in mitochondria (Pain & Dancis, 2016). Several mitochondrial proteins (including NFS1, ISCU, CISD1, and CISD2) require iron for iron-sulfur cluster biogenesis reactions for the negative regulation of ferroptosis (Yuan *et al.*, 2016; Alvarez *et al.*, 2017; Kim *et al.*, 2018; Du *et al.*, 2019). Moreover, elesclomol stimulates copper retention and the subsequent buildup of ROS via the degradation of ATP7A, which promotes ferroptosis in colorectal cancer cells (Gao *et al.*, 2021). Cuprizone, which is a copper chelator, regulates demyelination by the stimulation of ferroptosis and eventually leads to the loss of oligodendrocytes (Jhelum *et al.*, 2020). Therefore, an association between iron and copper metabolism has been well-established in scientific literature. These findings highlight the role of ferroptosis and cuproptosis as potential targets for the treatment of cancer.

In this study, a predictive model based on cuproptosis-related FRGs was built successfully to evaluate the prognosis of patients with BC and the predictive performance of the model was further validated. The findings of this study may enhance the effectiveness of individualized treatment and prognostic evaluations in patients with BC.

## MATERIALS AND METHODS

### Patient and gene set data collection

Clinical and RNA-sequencing data of 1097 BC patients were obtained from the cancer genome atlas (TCGA) database and 1053 patients containing complete clinical data including overall survival, age, gender, T stage, N stage, M stage, and TNM stage, were obtained after screening, while 44 patients who lacked complete clinical data were excluded. The intrinsic subtype was defined by PAM 50 (Parker *et al.*, 2009). Moreover, 1904 cases of RNA-sequencing and corresponding clinical data were obtained from the molecular taxonomy of breast cancer international consortium (METABRIC) database as the validation set for prognosis, and datasets GSE18728 and GSE87455 from gene expression omnibus (GEO) database were used to compare changes in risk score before and after neoadjuvant chemotherapy. Furthermore, 13 cuproptosis-related genes were obtained from the cuproptosis-related study (Tsvetkov *et al.*, 2022), and 259 FRGs were downloaded from the FerrDb website (Zhou & Bao, 2020).

### Identification and prognosis of cuproptosis-related FRGs

The correlation between the expression of cuproptosis-related genes and FRGs was determined using the Pearson correlation coefficients. The criteria used to identify cuproptosis-related FRGs was of $P$ value $<0.001$ and the absolute value of the Pearson correlation coefficient $>0.3(|R|>0.3)$. The univariate Cox regression analysis was used to screen the prognosis-related genes.

### Building and validation of a prognostic model

Based on the outcome of univariate Cox regression analysis, the least absolute shrinkage and selection operator (LASSO) regression method was used for the identification of the best survival-related genes via glmnet R package (Tibshirani, 1997; Wang & Liu, 2020). The prognostic risk score formula was created using the coefficients obtained from LASSO regression and the expression levels of genes. The formula can be mathematically represented as: Risk Score = $\sum$ corresponding regression coefficient * expression of the gene. The risk scores of the patients with BC were determined and the patients were grouped into two groups: the high-risk group and the low-risk group using the median risk score as the cutoff. The Kaplan-Meier survival analysis was used to demonstrate the presence of survival differences between the two groups. A receiver operator characteristic (ROC) curve via survivalROC R package was constructed to evaluate the effectiveness of the prognostic model and the METABRIC cohort was used for further validation.

### Establishment of a nomogram based on risk score and clinical characteristics

Univariate and multivariate COX regression analyses were used for the evaluation of risk scores and clinical characteristics as independent prognostic factors. A nomogram based on risk score and clinical characteristics was established to predict the probability of 3-, 5- and 10-year overall survival (OS) for patients with BC, and the performance of the nomogram was assessed by calibration curves.

### Functional enrichment analysis, protein-protein interaction (PPI), and gene set enrichment analysis (GSEA)

The Gene Ontology (GO) analysis was carried out for the identification of biological activities, molecular mechanisms, and cellular components via clusterprofiler R package. Additionally, the signaling pathways were observed using the Kyoto Encyclopedia of Genes and Genomes (KEGG) analysis. Cuproptosis-related FRGs were submitted to the STRING database (http://www.string-db.org/) for obtaining insights into PPI. The Cytoscape program was used to build and render PPI networks. Using the MCODE plug-in, the most important modules were selected based on MCODE score >5. GSEA was carried out to investigate potential enrichment pathways in the high- and low-risk groups. $P$ value $<0.05$ was considered statistically significant.

### Immune cell analysis

Different algorithms including CIBERSORT (Newman *et al.*, 2015), CIBERSORT-ABS, EPIC (Racle *et al.*, 2017), MCP-counter (Becht *et al.*, 2016), QUANTISEQ (Finotello *et al.*, 2019), TIMER (Li *et al.*, 2017), and XCELL (Aran *et al.*, 2017) were compared to assess the level of immune cell infiltration between the high- and low-risk groups. The correlation between immune cells and cuproptosis-related FRGs was identified by using the TIMER database. Potential immune checkpoints were obtained from scientific literature and differences in expression in immune checkpoints among high- and low-risk groups were explored using the ggpubr and limma packages.

### Drug sensitivity analysis

To compare the difference in drug sensitivity between the two groups, the half-maximal inhibitory concentration (IC50) of drugs was assessed by the pRRophetic

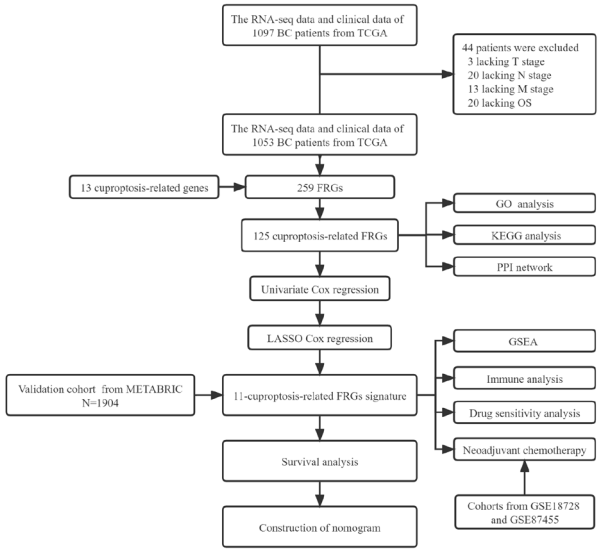


**Figure.1 Flow chart of this study.**

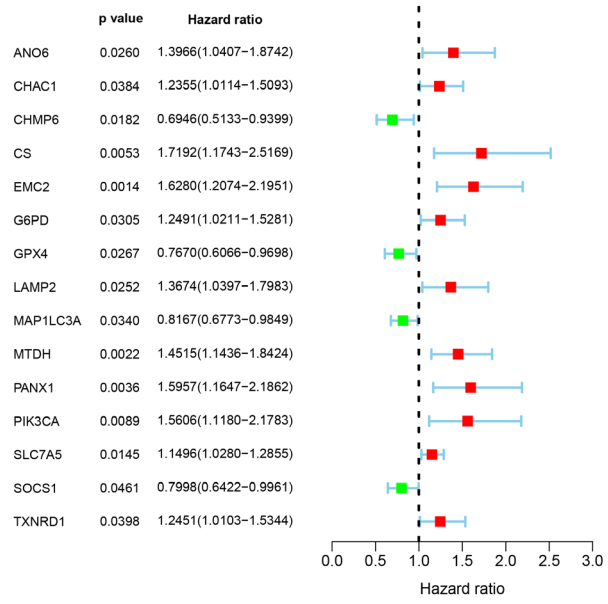


**Figure 2. Identification of prognostic cuproptosis-related FRGs. FRGs, ferroptosis-related genes.**

package. *P* value <0.05 was considered statistically significant.

### Statistics analysis

Statistical analysis was performed using R version 4.2.1. The Wilcoxon test was used to compare expression differences between the two groups. *P* value <0.05 was considered to be a statistically significant difference.

## RESULTS

### Identification of cuproptosis-related FRGs and their prognostic value in the TCGA cohort

The design of the study has been depicted using the flowchart (Fig. 1). A total of 125 FRGs were confirmed to be correlated with cuproptosis-related genes in the TCGA dataset (Supplementary Fig. S1 at https://ojs.ptbioch.edu.pl/index.php/abp/). Univariate Cox regression analysis was used to explore the prognostic value of these cuproptosis-related FRGs, and the results revealed that 15 genes had prognostic value (Fig. 2).

### Establishment and validation of cuproptosis-related FRG signature

Based on the 15 cuproptosis-related FRGs of prognostic value described above, LASSO Cox regression analysis was performed at the minimum λ value to create a risk model consisting of 11 genes (Supplementary Fig. S2 at https://ojs.ptbioch.edu.pl/index.php/abp/). The risk score for each patient was calculated using the following formula:

Risk Score = 0.187 * *ANO6* + 0.099 * *CHAC1* + (−0.075) * *CHMP6* + 0.115 * *CS* + 0.305 * *EMC2* + 0.195 * *G6PD* + (−0.024) * *GPX4* + 0.178 * *PANX1* + 0.055 * *PIK3CA* + 0.048 * *SLC7A5* + (−0.197) * *SOCS1*.

Patients with BC were divided into the high-risk group (n=526) and the low-risk group (n=527) based on the median risk score. Overall survival was significantly shorter in the high-risk group than in the low-risk group (*P*<0.001), suggesting a negative correlation between risk score and prognosis (Fig. 3A). Time-dependent ROC curve analysis verified the accuracy of the prognostic signature of patients with BC, with AUCs reaching 0.669 for 3 years, 0.643 for 5 years, and 0.711 for 10 years (Fig. 3B).

To verify the stability of the cuproptosis-related FRG signature, risk scores were calculated for patients in the METABRIC cohort by using the risk score formula ob-

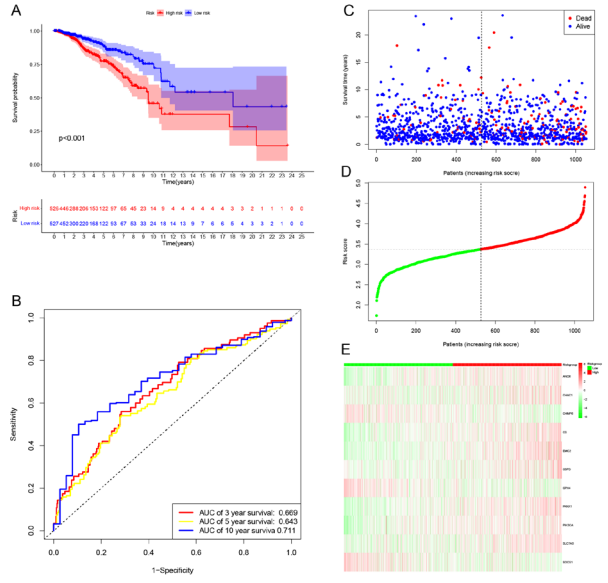


**Figure 3. Construction of the prognostic signature based on cuproptosis-related FRGs in TCGA cohort.**
(**A**) Kaplan-Meier curves for OS of BC patients between high-risk and low-risk groups. (**B**) Time-dependent ROC curves for OS. (**C**) Distribution of survival status based on the risk score. (**D**) The high-risk and low-risk groups were divided based on the median risk score. (**E**) Heatmap showed the difference in expression of 11 cuproptosis-related FRGs in high- and low-risk patients. BC, breast cancer; FRGs, ferroptosis-related genes; OS, overall survival; ROC, receiver operating characteristic; TCGA, the cancer genome atlas.

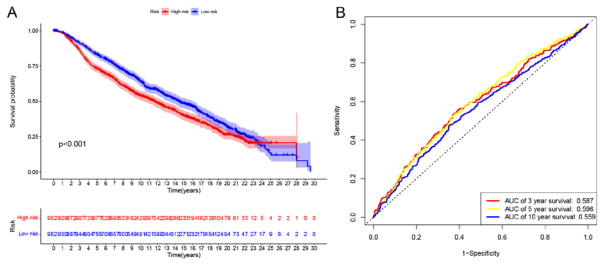


**Figure 4. Construction of the prognostic signature based on cuproptosis-related FRGs in METABRIC cohort.**
(**A**) Kaplan-Meier curves for OS of BC patients between high-risk and low-risk groups. (**B**) Time-dependent ROC curves for OS. BC, breast cancer; FRGs, ferroptosis-related genes; METABRIC, molecular taxonomy of breast cancer international consortium; OS, overall survival; ROC, receiver operating characteristic.

tained from the TCGA cohort. K-M survival analysis revealed a poor prognosis in the high-risk group (Fig. 4A, $P$<0.001). The result obtained was consistent with the TCGA dataset. The time-dependent ROC curves showed AUCs of 0.587 at 3 years, 0.596 at 5 years, and 0.559 at 10 years (Fig. 4B).

## The signature based on cuproptosis-related FRGs was an independent indicator of BC prognosis

For further assessment of the independent prognostic value of cuproptosis-related FRG signature, univariate and multivariate Cox regression analyses of clinical characteristics, including age, gender, and TNM stage were performed. Univariate analysis revealed that higher risk scores, T stage, N stage, and M stage were significantly associated with adverse OS in patients with BC (Fig. 5A), and negative estrogen receptor (ER) and progesterone receptor (PR) were suggestive of poor prognosis. The risk score, age, N stage, and M stage were shown to be independent risk factors for OS in the multivariate Cox analysis (Fig. 5B). Therefore, the cuproptosis-related FRG signature was an independent prognostic indicator for patients with BC.

## Association between the risk score and clinical characteristics

For the assessment of the impact of cuproptosis-related FRG signature in the development and progression of BC, the association between risk score and clinical characteristics was explored. Chi-square test analysis revealed significant differences between risk groups in T stage, N stage, TNM stage, PR, ER, human epidermal growth factor receptor (HER-2), and intrinsic subtype (Fig. 6). In addition, HER-2-enriched, ER-negative, PR-negative, HER-2-positive, higher N stage, and TNM stage indicated a higher risk score (Fig. 7). Stratified analysis was carried out for the identification of the prognostic value of the cuproptosis-related FRG signature in subgroups. The results revealed that this signature had significant prognostic efficacy in age <=65 ($P$=0.001), age >65 ($P$=0.009), female ($P$<0.001), T1 stage ($P$=0.011), T2-T4 stage ($P$=0.001), N0 stage ($P$<0.001), N1-N3 stage ($P$=0.018), M0 stage ($P$<0.001), stage I ($P$=0.047) and II-IV ($P$<0.001). However, no significant prognostic value was observed in the male patients and the M1 stages ($P$>0.05) (Fig. 8).

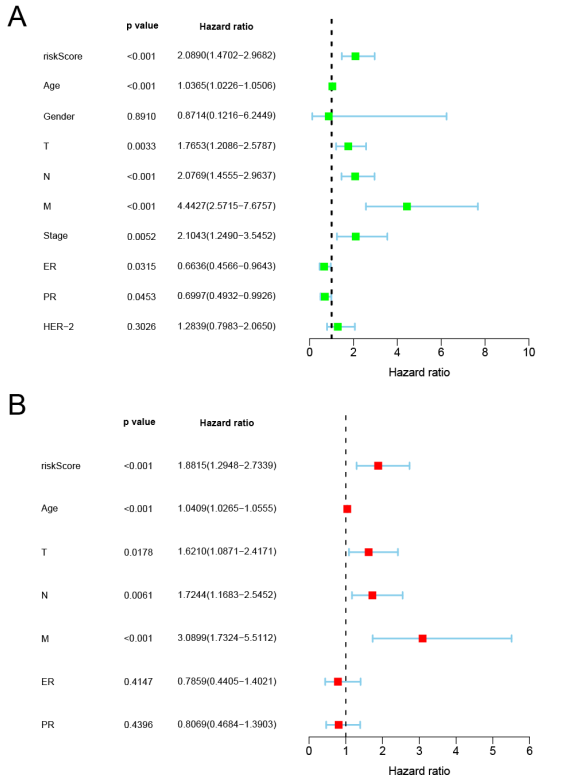


**Figure 5. Cuproptosis-related FRG signature was shown to be an independent risk factor for OS in TCGA.**
(**A**) Univariate Cox regression analysis between OS and various prognostic parameters. (**B**) Multivariate Cox regression analysis between OS and various prognostic parameters. FRG, ferroptosis-related gene; OS, overall survival; TCGA, the cancer genome atlas.

## Establishment of nomogram

A nomogram was constructed using risk score and clinical characteristics, including age, T stage, N stage, and M stage (Fig. 9A). The nomogram predicted the survival of BC patients at 3, 5, and 10 years. The calibration curves further validated the consistency of the actual OS of the patients with the predictions of the nomogram (Fig. 9B).


**Figure 6. Relationship between signature and clinical characteristics.**
* for $P$<0.05; *** for $P$<0.001.

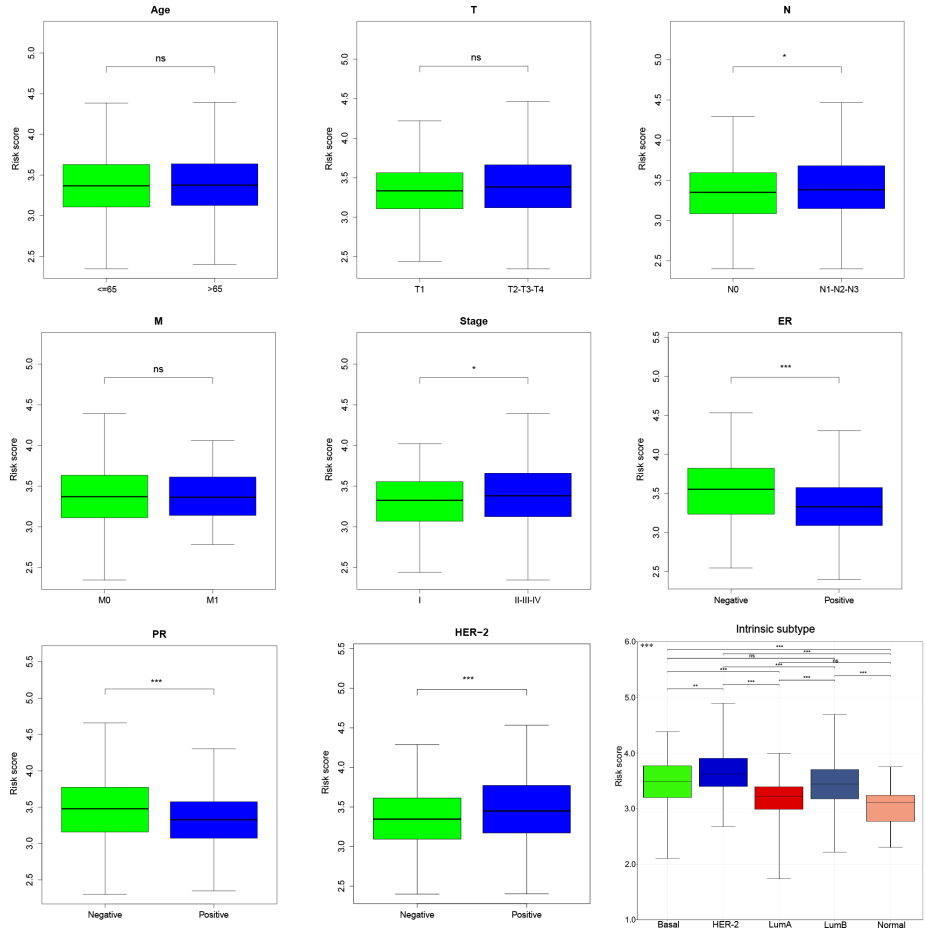


**Figure 7. Relationship between signature and clinical characteristics.**
ns for $P>0.05$; * for $P<0.05$; ** for $P<0.01$; *** for $P<0.001$.

## Functional enrichment and PPI of cuproptosis-related FRGs

The potential biological functions involved in 125 cuproptosis-related FRGs were analyzed using the GO and KEGG databases. GO analysis revealed the association of FRGs with biological processes like response to oxidative stress, cellular response to chemical stress, and response to nutrient levels (Supplementary Fig. S3A at https://ojs.ptbioch.edu.pl/index.php/abp/). In addition, in the KEGG pathway, the results revealed the involvement of FRGs in lipid and atherosclerosis, autophagy, FoxO signaling pathway, central carbon metabolism in cancer, and ferroptosis (Supplementary Fig. S3B at https://ojs.ptbioch.edu.pl/index.php/abp/). STRING database revealed that the PPI network of cuproptosis-related FRGs consisted of 125 nodes and 276 edges (Supplementary Fig. S3C at https://ojs.ptbioch.edu.pl/index.php/abp/). The most significant module consisted of 11 cuproptosis-related FRGs, including 11 nodes and 66 edges.

## GSEA

GSEA was used to further explore the potential mechanisms of cuproptosis-related FRG signature. The results revealed the enrichment of steroid biosynthesis, ABC transporters, base excision repair, glycosaminoglycan biosynthesis, other glycan degradation, and protein export in the high-risk group (Supplementary Fig. S3D at https://ojs.ptbioch.edu.pl/index.php/abp/). In contrast, ascorbate and aldarate metabolism, olfactory transduction, pentose and glucuronate interconversions, and systemic lupus erythematosus were mainly enriched in the low-risk group (Supplementary Fig. S3E at https://ojs.ptbioch.edu.pl/index.php/abp/).

## Immune infiltration level of cuproptosis-related FRG signature

The heatmap depicted the relationship between the cuproptosis-related FRG signature and immune cell subgroups according to the analysis of CIBERSORT, CIBERSORT-ABS, EPIC, MCP-counter, QUANTISEQ, TIMER, and XCELL algorithms (Fig. 10). The CIBERSORT result showed a higher proportion of CD4+ memory T cells, resting NK cells, M0 macrophages, M1 macrophages, M2 macrophages, eosinophils, and neutrophils in the high-risk group, whereas the low-risk group had higher proportions of memory B cells, CD8+ T cells, T follicular helper cells, Tregs, activated NK cells, monocytes, myeloid dendritic cells, activated mast cells, and resting mast cells (Supplementary Fig. S4 at https://ojs.ptbioch.edu.pl/index.php/abp/). In addition, the TIMER database was used to analyze the correlation between each FRG and immune cells. *ANO6*, *CS*, *EMC2*, *PANX1*, and *PIK3CA* were found to be positively correlated with multiple immune cells such as CD8+ T cells, macrophages, neutrophils, and dendritic cells. *CHAC1*, *SLC7A5*, and *SOCS1* were positively correlated with B cells, neutrophils, and dendritic cells. *CHMP6* was nega-

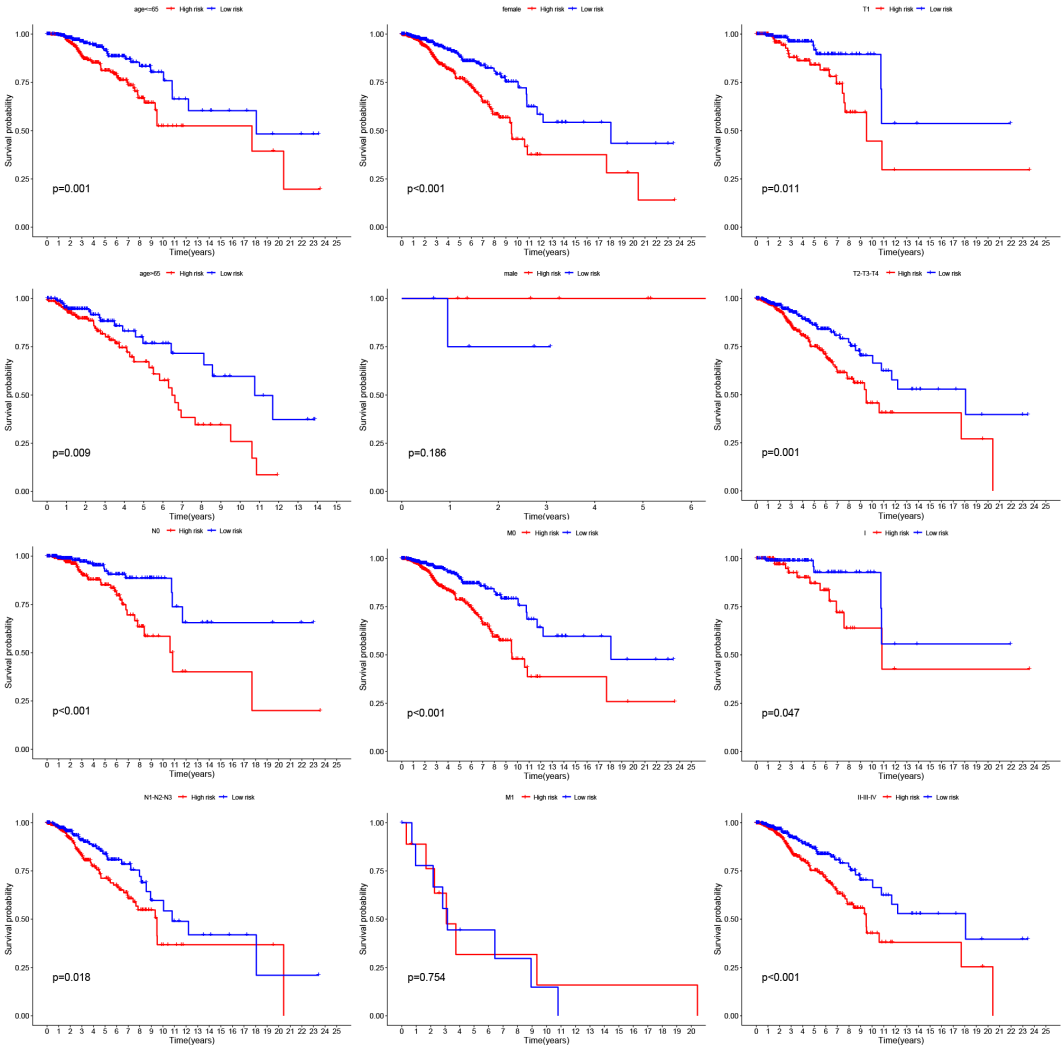


**Figure 8. Kaplan-Meier curves of OS differences between high- and low-risk groups stratified by age, gender, T stage, N stage, M stage or TNM stage. OS, overall survival.**

tively correlated with CD8+ T cells while positively correlated with CD4+ T cells. *GPX4* was negatively correlated with B cells, CD8+ T cells, macrophage, neutrophil, and dendritic cells. *G6PD* was positively correlated with B cells (Supplementary Fig. S5-6 at https://ojs.ptbioch.edu.pl/index.php/abp/).

Due to the importance of immunotherapy, the differences in immune checkpoints between risk score subgroups were analyzed. The results indicated higher expression of most immune checkpoints including *PDCD1*, *LAG3*, etc. in the low-risk group, suggesting a greater benefit of immune checkpoint suppression therapy in low-risk patients. The high expression of *CD80*, *PD-L2*, and *TNFSF4* in the high-risk group can aid in guiding the study for the optimization of immune checkpoint inhibitors (Fig. 11).

### Neoadjuvant chemotherapy and drug sensitivity analysis

To investigate whether the risk score of tumors changes during neoadjuvant chemotherapy. We used two chemotherapy BC cohorts. A significant reduction in risk score was observed in patients treated with docetaxel and capecitabine by comparing paired patients from GSE18728 (Fig. 12A). In the GSE87455 cohort treated with epirubicin and docetaxel, 69 paired patients who received two cycles of treatment had significantly lower risk score than before treatment (Fig. 12B). Meanwhile, 57 paired patients who received six cycles of treatment had significantly lower risk score than before treatment (Fig. 12C). To further optimize chemotherapy in patients with BC, potential antitumor drugs were screened to compare the differences in drug sensitivity between the high- and low-risk groups. The results of sensitivity analysis showed that the IC50 values of drugs including AUY922, docetaxel, etoposide, imatinib, mitomycin C, paclitaxel, and SL 0101-1 were significantly reduced in the low-risk group, suggesting a higher sensitivity of the patients in the low-risk group to these drugs (Fig. 13A-G). Patients in the high-risk group were found to be more sensitive to AKT inhibitor VIII and cisplatin (Fig. 13H-I).

## DISCUSSION

With the development of molecular diagnostic studies, medical professionals are increasingly resorting to the clinical practice of molecular diagnostics in BC, such as Oncotype dX and MammaPrint (Li *et al.*, 2017; Barzaman *et al.*, 2020). BC is a systemic disease and has

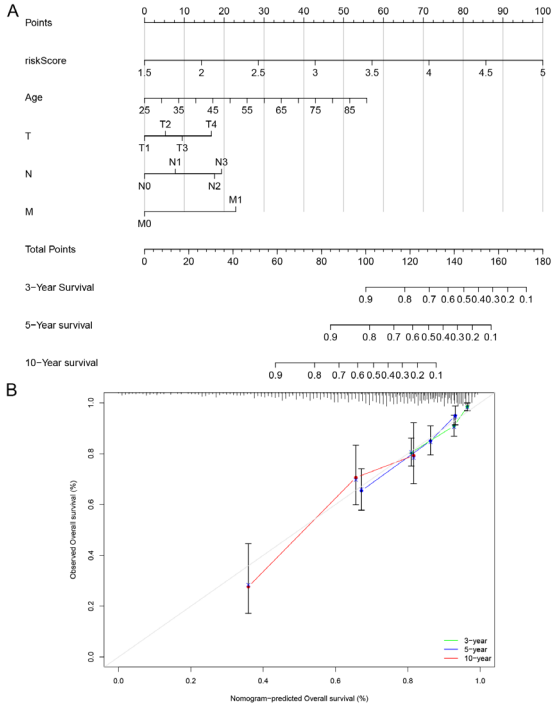


**Figure 9. Construction of a prognostic nomogram.**
(**A**) Nomogram of OS prediction with age, T stage, N stage, M stage and signature as parameters. (**B**) The calibration curves of the nomogram for 3-, 5-, and 10-year OS prediction. OS, overall survival.

evolved from the conventional surgical treatment to the current combination therapy including radiotherapy, chemotherapy, hormonal therapy, and biological therapy (Ben-Dror *et al.*, 2022). Patients with BC may have to choose among different options for postoperative systemic therapy. Therefore, it is imperative to find more effective biomarkers to adapt adjuvant therapies to individualize treatment for patients.

To the best of our knowledge, this is the first study to explore the correlation between FRGs and cuproptosis-related genes in patients with BC. Unlike other regulatory cell death processes, cuproptosis is primarily associated with adiposity of the tricarboxylic acid cycle and involves the loss of iron-sulfur cluster proteins and induction of ROS (Li *et al.*, 2022; Tsvetkov *et al.*, 2022). Gao and others (Gao *et al.*, 2021) reported the accumulation of ROS due to copper retention, which inhibited the *SLC7A11* levels, thereby enhancing oxidative stress and ferroptotic cell death in colorectal cancer. Thus, FRGs

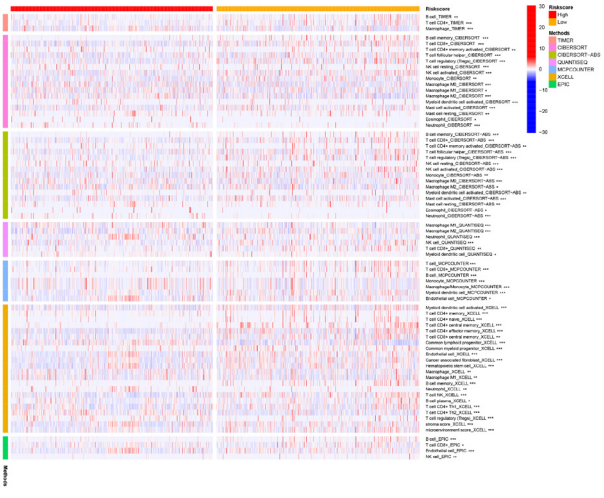

**Figure 10. Analysis of immune cells between high- and low-risk groups.**
* for $P<0.05$; ** for $P<0.01$; *** for $P<0.001$.

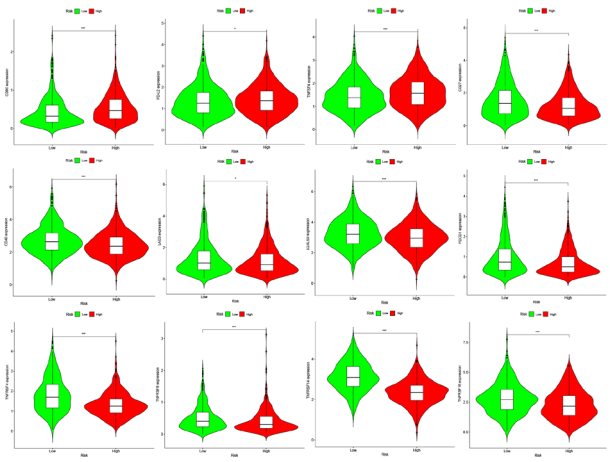

**Figure 11. Differences in immune checkpoints between the high- and low-risk groups.**
* for $P<0.05$; *** for $P<0.001$.

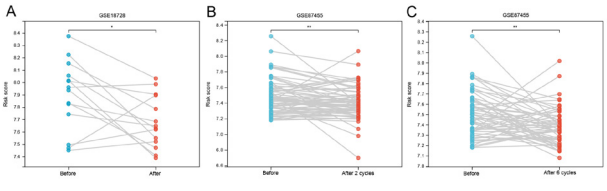


**Figure 12. Pairwise comparison of risk score in GSE18728, GSE87455 by pre-chemotherapy and post-chemotherapy.**
* for $P<0.05$; ** for $P<0.01$.

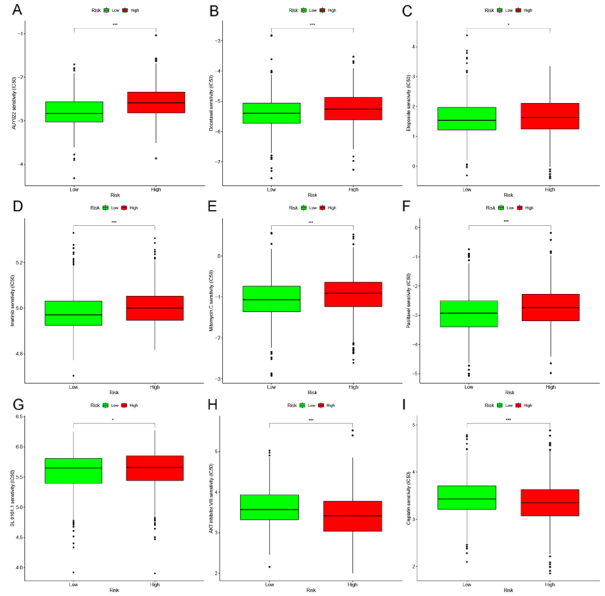


**Figure 13. Sensitivity analysis of antitumor drugs between high-risk and low-risk groups.**
(**A**) AUY922; (**B**) docetaxel; (**C**) etoposide; (**D**) imatinib; (**E**) mitomycin C; (**F**) paclitaxel; (**G**) SL 0101-1; (**H**) AKT inhibitor VIII; (**I**) cisplatin. * for $P<0.05$; *** for $P<0.001$.

may cause regulated cell death through the cuproptosis-related mechanism.

In this study, the relationship between 259 FRGs and 13 cuproptosis-related genes in BC was comprehensively evaluated and screened for cuproptosis-related FRGs. The relationship between cuproptosis-related FRGs and OS in BC was analyzed and a novel prognostic model containing 11 cuproptosis-related FRGs was constructed. The accuracy of the model was verified by the METABRIC cohort. Survival and ROC analyses revealed a good predictive ability of the model. Univariate and multivariate Cox analysis established the risk score of cuproptosis-related FRG signature to be an independent prognostic indicator for BC. The risk score was further found to be correlated with immune infiltrating cells and the expression of immune checkpoints between risk subgroups was analyzed. Finally, two neoadjuvant chemotherapy cohorts were used to show that the risk score was significantly reduced over the course of treatment, and nine antitumor drugs were screened for the treatment of patients with BC in different risk subgroups.

A significant difference between cuproptosis-related FRG signature and the clinical stage was observed, suggesting that higher risk scores were concentrated in more advanced tumor stages, ER-negative, PR-negative, and HER-2-positive, which further validates the poorer prognosis in the high-risk group. Meanwhile, the prognosis of cuproptosis-related FRG signature was confirmed in different subgroups with different clinical characteristics, except for male patients and patients with distant metastases, which could be because of the small sample size in these two subgroups. Therefore, the proposed model has demonstrated generalizability in different strata of patients with BC.

The cuproptosis-related FRG signature included *ANO6*, *CHAC1*, *CHMP6*, *CS*, *EMC2*, *G6PD*, *GPX4*, *PANX1*, *PIK3CA*, *SLC7A5*, and *SOCS1*. These genes included ferroptosis driver genes (*ANO6*, *CHAC1*, *CS*, *EMC2*, *G6PD*, *PANX1*, and *PIK3CA*) and ferroptosis suppressor genes (*CHMP6*, *PGX4*, and *SOCS1*). Currently, SLC7A5 is an unclassified regulator whose role in ferroptosis is unclear. There is growing evidence of the involvement of *ANO6* in multiple forms of cell death, including necroptosis, pyroptosis, and ferroptosis (Ousingsawat *et al.*, 2017; Ousingsawat *et al.*, 2018; Simões *et al.*, 2018). As a non-selective $Ca^{2+}$ -activated ion channel, lipid scramblase *ANO6* plays a critical role in the induction of ferroptotic cell death by disrupting the stability of membrane phospholipids (Ousingsawat *et al.*, 2019). Chen et al. reported that *CHAC1* contributes to cystine starvation and thereby induces ferroptotic cell death in triple-negative BC cells via the GCN2-eIF2α-ATF4 pathway (Chen *et al.*, 2017). Overexpression of CHAC1 has been linked to the enhanced sensitivity of prostate cancer cells to docetaxel, but the effect was reversed after co-treatment with ferroptosis inhibitors, suggesting that *CHAC1* functions as a potential therapeutic target for castration-resistant prostate cancer by inducing ferroptotic cell death (He *et al.*, 2021). Ferroptosis activators such as erastin and RSL3 increased *CHMP6* accumulation by triggering calcium influx. Silencing of *CHMP6* expression sensitized cancer cells to lipid peroxidation-mediated ferroptosis but did not affect iron accumulation (Dai *et al.*, 2020). *CS* increased the accumulation of citrate in hypoxic triple-negative BC cells, which promoted the migration and invasion of cancer cells (Peng *et al.*, 2019). The overexpression of *G6PD* suggests a poor prognosis in hepatocellular carcinoma and inhibits ferroptotic cell death of the tumor by targeting cytochrome oxidoreductase (Cao *et al.*, 2021). Luo et al. reported the resistance of *G6PD* for doxorubicin-induced apoptosis in triple-negative BC cells by the maintenance of high glutathione levels (Luo *et al.*, 2022). Genetic models were used for the identification of *GPX4* as a key regulator of ferroptosis and that inhibition of GPX4-induced ferroptosis enhanced the sensitivity of triple-negative BC cells to gefitinib (Seibt *et al.*, 2019; Song *et al.*, 2020). A recent study reported that high expression of *PANX1* induced local immunosuppression in tumor microenvironment of basal-like BC, as evidenced by high infiltration levels of neutrophils and adenosine production (Chen *et al.*, 2022). *SLC7A5* supported the proliferation and growth of tumor cells by increasing mTORC1 activity through the upregulation of regulatory transcription factors under hypoxic conditions (Nachef *et al.*, 2021). In addition, *SLC7A5* inhibitors were used to treat patients with advanced biliary tract cancer such that no disease progression occurred for two years (Hayes *et al.*, 2015). *SOCS1* sensitizes cells to ferroptosis by the activation of p53 target gene expression and glutathione level reduction (Saint-Germain *et al.*, 2017).

The results of GO analysis and KEGG pathway analysis revealed the relation of 125 cuproptosis-related FRGs to certain biological functions or pathways, such as response to oxidative stress, cellular response to chemical stress, autophagy, FoxO signaling pathway, and central carbon metabolism in cancer. Therefore, lipid peroxidation, a key to the induction of ferroptosis, is mediated by oxidative and antioxidant systems, along with autophagy (Chen *et al.*, 2021).

Tumor-associated macrophages have been shown to promote tumor invasion in BC by promoting angiogenesis and remodeling the tumor extracellular matrix while evading the host immune response and suppressing the antitumor effects of cytotoxic T cells (Choi *et al.*, 2018; Mehta *et al.*, 2021). The results of this study revealed higher levels of macrophage infiltration in the high-risk group, accrediting the poor prognosis in the high-risk group to the immunosuppression of the tumor microenvironment. It was also found that patients in the low-risk group had a higher likelihood of benefitting from immunotherapy, while patients in the high-risk group may be more sensitive to immunosuppressive agents targeting *CD80*, *PD-L2*, and *TNFSF4*. Risk score was found to become lower after treatment through the neoadjuvant cohort, which may suggest a remission of the tumor. Finally, the sensitivity of high- and low-risk groups to different antitumor drugs was explored and results revealed that patients in the high-risk group were more sensitive to AKT inhibitor VIII and cisplatin. The results obtained from this study combined with the data available in the literature will aid the facilitation of the optimization of chemotherapy regimens for patients with BC.

However, the objects of this study were from public databases, and clinical data is essential for further validation. Although 125 cuproptosis-related FRGs have been identified, the correlation between FRGs and cuproptosis-related genes was not established. Finally, subgroup-related pathways, immune infiltration, and drug sensitivity require further experimental validation.

## Declarations

**Acknowledgements.** We thank Bullet Edits Limited for the linguistic editing and proofreading of the manuscript.

**Author contributions.** QZ and XZ contributed to this study's design, data analysis, and manuscript prep-

aration. The authors have read and approved the final manuscript.

**Availability of data.** The raw data of this study are derived from the TCGA database (https://portal.gdc.cancer.gov/), GEO database (https://www.ncbi.nlm.nih.gov/geo/) and METABRIC database (http://www.cbioportal.org/study/summary?id=brca_metabric), which are publicly available databases.

**Code availability.** The code used in this study are available from the corresponding author on reasonable request.

**Conflict of interests.** The authors declare that there is no conflict of interest regarding the publication of this paper.

## REFERENCES


Alvarez SW, Sviderskiy VO, Terzi EM, Papagiannakopoulos T, Moreira AL, Adams S, Sabatini DM, Birsoy K, Possemato R (2017) NFS1 undergoes positive selection in lung tumours and protects cells from ferroptosis. *Nature* **551**: 639–643. https://doi.org/10.1038/nature24637

Aran D, Hu Z, Butte AJ (2017) xCell: digitally portraying the tissue cellular heterogeneity landscape. *Genome Biol* **18**: 220. https://doi.org/10.1186/s13059-017-1349-1

Azamjah N, Soltan-Zadeh Y, Zayeri F (2019) Global trend of breast cancer mortality rate: a 25-year study. *Asian Pac J Cancer Prev* **20**: 2015–2020. https://doi.org/10.31557/APJCP.2019.20.7.2015

Barzaman K, Karami J, Zarei Z, Hosseinzadeh A, Kazemi MH, Moradi-Kalbolandi S, Safari E, Farahmand L (2020) Breast cancer: Biology, biomarkers, and treatments. *Int Immunopharmacol* **84**: 106535. https://doi.org/10.1016/j.intimp.2020.106535

Becht E, Giraldo NA, Lacroix L, Buttard B, Elarouci N, Petitprez F, Selves J, Laurent-Puig P, Sautès-Fridman C, Fridman WH, de Reyniès A (2016) Estimating the population abundance of tissue-infiltrating immune and stromal cell populations using gene expression. *Genome Biol* **17**: 218. https://doi.org/10.1186/s13059-016-1070-5

Ben-Dror J, Shalamov M, Sonnenblick A (2022) The History of Early Breast Cancer Treatment. *Genes (Basel)* **13**. https://doi.org/10.3390/genes13060960

Cao F, Luo A, Yang C (2021) G6PD inhibits ferroptosis in hepatocellular carcinoma by targeting cytochrome P450 oxidoreductase. *Cell Signal* **87**: 110098. https://doi.org/10.1016/j.cellsig.2021.110098

Caswell-Jin JL, Plevritis SK, Tian L, Cadham CJ, Xu C, Stout NK, Sledge GW, Mandelblatt JS, Kurian AW (2018) Change in survival in metastatic breast cancer with treatment advances: meta-analysis and systematic review. *JNCI Cancer Spectr* **2**: pky062. https://doi.org/10.1093/jncics/pky062

Chen MS, Wang SF, Hsu CY, Yin PH, Yeh TS, Lee HC, Tseng LM (2017) CHAC1 degradation of glutathione enhances cystine-starvation-induced necroptosis and ferroptosis in human triple negative breast cancer cells via the GCN2-eIF2α-ATF4 pathway. *Oncotarget* **8**: 114588–114602. https://doi.org/10.18632/oncotarget.23055

Chen W, Li B, Jia F, Li J, Huang H, Ni C, Xia W (2022) High PANX1 expression leads to neutrophil recruitment and the formation of a high adenosine immunosuppressive tumor microenvironment in basal-like breast cancer. *Cancers (Basel)* **14**. https://doi.org/10.3390/cancers14143369

Chen X, Kang R, Kroemer G, Tang D (2021) Broadening horizons: the role of ferroptosis in cancer. *Nat Rev Clin Oncol* **18**: 280–296. https://doi.org/10.1038/s41571-020-00462-0

Choi J, Gyamfi J, Jang H, Koo JS (2018) The role of tumor-associated macrophage in breast cancer biology. *Histol Histopathol* **33**: 133–145. https://doi.org/10.14670/HH-11-916

Dai E, Meng L, Kang R, Wang X, Tang D (2020) ESCRT-III-dependent membrane repair blocks ferroptosis. *Biochem Biophys Res Commun* **522**: 415–421. https://doi.org/10.1016/j.bbrc.2019.11.110

DeSantis CE, Ma J, Gaudet MM, Newman LA, Miller KD, Goding Sauer A, Jemal A, Siegel RL (2019) Breast cancer statistics, 2019. *CA Cancer J Clin* **69**: 438–451. https://doi.org/10.3322/caac.21583

Dixon SJ, Lemberg KM, Lamprecht MR, Skouta R, Zaitsev EM, Gleason CE, Patel DN, Bauer AJ, Cantley AM, Yang WS, Morrison B 3rd, Stockwell BR (2012) Ferroptosis: an iron-dependent form of nonapoptotic cell death. *Cell* **149**: 1060–1072. https://doi.org/10.1016/j.cell.2012.03.042

Du J, Wang T, Li Y, Zhou Y, Wang X, Yu X, Ren X, An Y, Wu Y, Sun W, Fan W, Zhu Q, Wang Y, Tong X (2019) DHA inhibits proliferation and induces ferroptosis of leukemia cells through autophagy dependent degradation of ferritin. *Free Radic Biol Med* **131**: 356–369. https://doi.org/10.1016/j.freeradbiomed.2018.12.011

Feng Y, Spezia M, Huang S, Yuan C, Zeng Z, Zhang L, Ji X, Liu W, Huang B, Luo W, Liu B, Lei Y, Du S, Vuppalapati A, Luu HH, Haydon RC, He TC, Ren G (2018) Breast cancer development and progression: Risk factors, cancer stem cells, signaling pathways, genomics, and molecular pathogenesis. *Genes Dis* **5**: 77–106. https://doi.org/10.1016/j.gendis.2018.05.001

Finotello F, Mayer C, Plattner C, Laschober G, Rieder D, Hackl H, Krogsdam A, Loncova Z, Posch W, Wilflingseder D, Sopper S, Ijsselsteijn M, Brouwer TP, Johnson D, Xu Y, Wang Y, Sanders ME, Estrada MV, Ericsson-Gonzalez P, Charoentong P, Balko J, de Miranda NFDCC, Trajanoski Z (2019) Molecular and pharmacological modulators of the tumor immune contexture revealed by deconvolution of RNA-seq data. *Genome Med* **11**: 34. https://doi.org/10.1186/s13073-019-0638-6

Friedmann Angeli JP, Krysko DV, Conrad M (2019) Ferroptosis at the crossroads of cancer-acquired drug resistance and immune evasion. *Nat Rev Cancer* **19**: 405–414. https://doi.org/10.1038/s41568-019-0149-1

Gao W, Huang Z, Duan J, Nice EC, Lin J, Huang C (2021) Elesclomol induces copper-dependent ferroptosis in colorectal cancer cells *via* degradation of ATP7A. *Mol Oncol* **15**: 3527–3544. https://doi.org/10.1002/1878-0261.13079

Hassannia B, Vandenabeele P, Vanden Berghe T (2019) Targeting ferroptosis to iron out cancer. *Cancer Cell* **35**: 830–849. https://doi.org/10.1016/j.ccell.2019.04.002

Hayes GM, Chinn L, Cantor JM, Cairns B, Levashova Z, Tran H, Velilla T, Duey D, Lippincott J, Zachwieja J, Ginsberg MH, H van der Horst E (2015) Antitumor activity of an anti-CD98 antibody. *Int J Cancer* **137**: 710–720. https://doi.org/10.1002/ijc.29415

He S, Zhang M, Ye Y, Zhuang J, Ma X, Song Y, Xia W (2021) ChaC glutathione specific γ-glutamylcyclotransferase 1 inhibits cell viability and increases the sensitivity of prostate cancer cells to docetaxel by inducing endoplasmic reticulum stress and ferroptosis. *Exp Ther Med* **22**: 997. https://doi.org/10.3892/etm.2021.10429

Huang L, McClatchy DB, Maher P, Liang Z, Diedrich JK, Soriano-Castell D, Goldberg J, Shokhirev M, Yates JR 3rd, Schubert D, Currais A (2020) Intracellular amyloid toxicity induces oxytosis/ferroptosis regulated cell death. *Cell Death Dis* **11**: 828. https://doi.org/10.1038/s41419-020-03020-9

Jhelum P, Santos-Nogueira E, Teo W, Haumont A, Lenoël I, Stys PK, David S (2020) Ferroptosis mediates cuprizone-induced loss of oligodendrocytes and demyelination. *J Neurosci* **40**: 9327–9341. https://doi.org/10.1523/JNEUROSCI.1749-20.2020

Jiang Y, Huo Z, Qi X, Zuo T, Wu Z (2022) Copper-induced tumor cell death mechanisms and antitumor theragnostic applications of copper complexes. *Nanomedicine (Lond)* **17**: 303–324. https://doi.org/10.2217/nnm-2021-0374

Kahlson MA, Dixon SJ (2022) Copper-induced cell death. *Science* **375**: 1231–1232. https://doi.org/10.1126/science.abo3959

Kim EH, Shin D, Lee J, Jung AR, Roh JL (2018) CISD2 inhibition overcomes resistance to sulfasalazine-induced ferroptotic cell death in head and neck cancer. *Cancer Lett* **432**: 180–190. https://doi.org/10.1016/j.canlet.2018.06.018

Li G, Hu J, Hu G (2017) Biomarker studies in early detection and prognosis of breast cancer. *Adv Exp Med Biol* **1026**: 27–39. https://doi.org/10.1007/978-981-10-6020-5_2

Li SR, Bu LL, Cai L (2022) Cuproptosis: lipoylated TCA cycle proteins-mediated novel cell death pathway. *Signal Transduct Target Ther* **7**: 158. https://doi.org/10.1038/s41392-022-01014-x

Li T, Fan J, Wang B, Traugh N, Chen Q, Liu JS, Li B, Liu XS (2017) TIMER: A web server for comprehensive analysis of tumor-infiltrating immune cells. *Cancer Res* **77**: e108–e110. https://doi.org/10.1158/0008-5472.CAN-17-0307

Loibl S, Poortmans P, Morrow M, Denkert C, Curigliano G (2021) Breast cancer. *Lancet* **397**: 1750–1769. https://doi.org/10.1016/S0140-6736(20)32381-3

Luo M, Fu A, Wu R, Wei N, Song K, Lim S, Luo KQ (2022) High expression of G6PD increases doxorubicin resistance in triple negative breast cancer cells by maintaining GSH level. *Int J Biol Sci* **18**: 1120–1133. https://doi.org/10.7150/ijbs.65555

Mehta AK, Kadel S, Townsend MG, Oliwa M, Guerriero JL (2021) Macrophage biology and mechanisms of immune suppression in breast cancer. *Front Immunol* **12**: 643771. https://doi.org/10.3389/fimmu.2021.643771

Nachef M, Ali AK, Almutairi SM, Lee SH (2021) Targeting SLC1A5 and SLC3A2/SLC7A5 as a potential strategy to strengthen anti-tumor immunity in the tumor microenvironment. *Front Immunol* **12**: 624324. https://doi.org/10.3389/fimmu.2021.624324

Newman AM, Liu CL, Green MR, Gentles AJ, Feng W, Xu Y, Hoang CD, Diehn M, Alizadeh AA (2015) Robust enumeration of cell subsets from tissue expression profiles. *Nat Methods* **12**: 453–457. https://doi.org/10.1038/nmeth.3337

Ousingsawat J, Cabrita I, Wanitchakool P, Sirianant L, Krautwald S, Linkermann A, Schreiber R, Kunzelmann K (2017) $Ca^{2+}$ signals, cell membrane disintegration, and activation of TMEM16F during

necroptosis. *Cell Mol Life Sci* **74**: 173–181. https://doi.org/10.1007/s00018-016-2338-3

Ousingsawat J, Schreiber R, Kunzelmann K (2019) TMEM16F/Anoctamin 6 in Ferroptotic Cell Death. *Cancers (Basel)* **11**. https://doi.org/10.3390/cancers11050625

Ousingsawat J, Wanitchakool P, Schreiber R, Kunzelmann K (2018) Contribution of TMEM16F to pyroptotic cell death. *Cell Death Dis* **9**: 300. https://doi.org/10.1038/s41419-018-0373-8

Pain D, Dancis A (2016) Roles of Fe-S proteins: from cofactor synthesis to iron homeostasis to protein synthesis. *Curr Opin Genet Dev* **38**: 45–51. https://doi.org/10.1016/j.gde.2016.03.006

Parker JS, Mullins M, Cheang MC, Leung S, Voduc D, Vickery T, Davies S, Fauron C, He X, Hu Z, Quackenbush JF, Stijleman IJ, Palazzo J, Marron JS, Nobel AB, Mardis E, Nielsen TO, Ellis MJ, Perou CM, Bernard PS (2009) Supervised risk predictor of breast cancer based on intrinsic subtypes. *J Clin Oncol* **27**: 1160–1167. https://doi.org/10.1200/JCO.2008.18.1370

Peng M, Yang D, Hou Y, Liu S, Zhao M, Qin Y, Chen R, Teng Y, Liu M (2019) Intracellular citrate accumulation by oxidized ATM-mediated metabolism reprogramming via PFKP and CS enhances hypoxic breast cancer cell invasion and metastasis. *Cell Death Dis* **10**: 228. https://doi.org/10.1038/s41419-019-1475-7

Racle J, de Jonge K, Baumgaertner P, Speiser DE, Gfeller D (2017) Simultaneous enumeration of cancer and immune cell types from bulk tumor gene expression data. *Elife* **6**. https://doi.org/10.7554/eLife.26476

Saint-Germain E, Mignacca L, Vernier M, Bobbala D, Ilangumaran S, Ferbeyre G (2017) SOCS1 regulates senescence and ferroptosis by modulating the expression of p53 target genes. *Aging (Albany NY)* **9**: 2137–2162. https://doi.org/10.18632/aging.101306

Seibt TM, Proneth B, Conrad M (2019) Role of GPX4 in ferroptosis and its pharmacological implication. *Free Radic Biol Med* **133**: 144–152. https://doi.org/10.1016/j.freeradbiomed.2018.09.014

Simões F, Ousingsawat J, Wanitchakool P, Fonseca A, Cabrita I, Benedetto R, Schreiber R, Kunzelmann K (2018) CFTR supports cell death through ROS-dependent activation of TMEM16F (anoctamin 6). *Pflugers Arch* **470**: 305–314. https://doi.org/10.1007/s00424-017-2065-0

Song X, Wang X, Liu Z, Yu Z (2020) Role of GPX4-mediated ferroptosis in the sensitivity of triple negative breast cancer cells to gefitinib. *Front Oncol* **10**: 597434. https://doi.org/10.3389/fonc.2020.597434

Sung H, Ferlay J, Siegel RL, Laversanne M, Soerjomataram I, Jemal A, Bray F (2021) Global Cancer Statistics 2020: GLOBOCAN Estimates of Incidence and Mortality Worldwide for 36 Cancers in 185 Countries. *CA Cancer J Clin* **71**: 209–249. https://doi.org/10.3322/caac.21660

Tibshirani R (1997) The lasso method for variable selection in the Cox model. *Stat Med* **16**: 385–395. https://doi.org/10.1002/(sici)1097-0258(19970228)16:4<385::aid-sim380>3.0.co;2-3

Tsvetkov P, Coy S, Petrova B, Dreishpoon M, Verma A, Abdusamad M, Rossen J, Joesch-Cohen L, Humeidi R, Spangler RD, Eaton JK, *et al.* (2022) Copper induces cell death by targeting lipoylated TCA cycle proteins. *Science* **375**: 1254–1261. https://doi.org/10.1126/science.abf0529

Waldron KJ, Rutherford JC, Ford D, Robinson NJ (2009) Metalloproteins and metal sensing. *Nature* **460**: 823–830. https://doi.org/10.1038/nature08300

Wang W, Liu W (2020) Integration of gene interaction information into a reweighted Lasso-Cox model for accurate survival prediction. *Bioinformatics* **36**: 5405–5414. https://doi.org/10.1093/bioinformatics/btaa1046

Wang Y, Wei Z, Pan K, Li J, Chen Q (2020) The function and mechanism of ferroptosis in cancer. *Apoptosis* **25**: 786–798. https://doi.org/10.1007/s10495-020-01638-w

Yuan H, Li X, Zhang X, Kang R, Tang D (2016) CISD1 inhibits ferroptosis by protection against mitochondrial lipid peroxidation. *Biochem Biophys Res Commun* **478**: 838–844. https://doi.org/10.1016/j.bbrc.2016.08.034

Zhang C, Liu X, Jin S, Chen Y, Guo R (2022) Ferroptosis in cancer therapy: a novel approach to reversing drug resistance. *Mol Cancer* **21**: 47. https://doi.org/10.1186/s12943-022-01530-y

Zhao L, Zhou X, Xie F, Zhang L, Yan H, Huang J, Zhang C, Zhou F, Chen J, Zhang L (2022) Ferroptosis in cancer and cancer immunotherapy. *Cancer Commun (Lond)* **42**: 88–116. https://doi.org/10.1002/cac2.12250

Zhou N, Bao J (2020) FerrDb: a manually curated resource for regulators and markers of ferroptosis and ferroptosis-disease associations. *Database (Oxford)* **2020**. https://doi.org/10.1093/database/baaa021